JHEP

Published for SISSA by Springer

Received: December 16, 2015
Revised: May 20, 2016
Accepted: June 20, 2016
Published: June 27, 2016

JHEP06(2016)156

The galactic center excess from $\mathbb{Z}_3$ scalar semi-annihilations

Yi Cai[a] **and Andrew Spray**[b]

[a] *ARC Centre of Excellence for Particle Physics at the Terascale, School of Physics, The University of Melbourne, Victoria 3010, Australia*

[b] *Center for Theoretical Physics of the Universe, Institute for Basic Science (IBS), Daejeon, 34051, Korea*

E-mail: yi.cai@unimelb.edu.au, a.spray.work@gmail.com

Abstract: We investigate the possibility of the $\mathbb{Z}_3$ scalar singlet model explaining the Fermi galactic centre excess. We find a good fit to the measured spectral excess in the region where the dark matter mass is comparable to the Higgs and the Higgs portal coupling $\lambda_{\rm HS} \sim 0.04$. This preferred region is consistent with constraints from vacuum stability and current dark matter experiments, and will be discovered or falsified soon by future dark matter direct detection experiment.

Keywords: Beyond Standard Model, Discrete Symmetries

ArXiv ePrint: 1511.09247

doi:10.1007/JHEP06(2016)156

Contents

JHEP06(2016)156

1 Introduction

The nature of dark matter (DM) is one of the biggest questions in contemporary particle physics. Despite intense efforts at many different experiments, no *unambiguous* non-gravitational signal has been found. However, current and near future experiments offer the prospect of decisively testing the weakly-interacting massive particle (WIMP) hypothesis. This makes experimental excesses more theoretically attractive now than in the past.

One of the most interesting recent anomalies in dark matter searches is the γ-ray galactic centre excess (GCE) discovered in Fermi data after subtraction of backgrounds. The original discovery [1] has been corroborated by several theoretical analyses [2–7], and recently by the Fermi collaboration itself [8]. The GCE has many of the features expected of DM annihilation into Standard Model (SM) states: the morphology in the sky matches what is expected from DM density distributions, and the required cross sections are very close to that of the canonical thermal WIMP. The spectrum is easily fit by various SM final states; $b\bar{b}$ for DM masses of 30–60 GeV offers the best fit, but Higgs, gauge boson and top final states with larger DM masses are also acceptable [7, 9, 10] . This has inspired considerable model building efforts to explain the observed signal [11–31]. Alternative explanations have been advanced, including pulsars [32–38] or cosmic rays at the galactic centre [39–41], but the efficacy of these explanations is contested [5, 42–44]. It is worth noting that the studies of refs. [37, 38] find evidence for a point source origin of the GCE. In any case, we find it interesting to consider a DM interpretation of this signal.

Semi-annihilation (SA) is a generic feature in DM phenomenology that occurs whenever DM is stabilized by a symmetry larger than $\mathbb{Z}_2$.It specifically modifies the relic density and indirect detection signals, which makes it interesting for interpreting the GCE. We compare SA and ordinary DM annihilation in figure 1. SA is characterised by non-decay processes with an odd number of external dark-sector states. In addition to enabling different final states and kinematics, SA is also irrelevant for collider and dark matter searches. This can allow strong indirect signals while weakening other constraints.

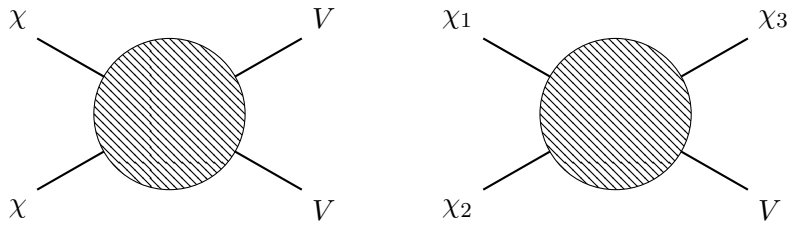

Figure 1. DM annihilation (left) and SA (right), where χ (V) is a dark (visible) sector field.

In a previous work [45], we showed that SA in a two-component DM model could explain the GCE through processes where a single Higgs is produced nearly at rest.[1] The subsequent decay of the Higgs to $b\bar{b}$ produces a spectrum very similar to annihilation of 60 GeV DM to the same final state. The dark sector only coupled to the SM through the Higgs portal, and SA played two essential roles related to this interatction. With SA significantly contributing to setting the thermal relic density, smaller Higgs portal couplings were allowed, thereby alleviating the stringent constraints from LUX. Additionally, DM annihilating through the Higgs portal will always preferentially produce gauge bosons over Higgses, resulting in a poorer fit to the GCE γ-ray spectrum. A large SA cross section substantially enhances the production rate of Higgses in our model.

In this paper, we apply the same approach to the simplest SA model: the $\mathbb{Z}_3$ scalar singlet model (Z3SSM) [49]. This model extends the SM by a single DM particle only, coupled renormalisably to the visible sector through the Higgs portal. It is also a minimal extension of the well-studied $\mathbb{Z}_2$ scalar singlet model [50]. The benefits that SA brought in our previous model apply also to the Z3SSM: weakening the direct detection bounds and enhancing the production rate of Higgses. The Z3SSM is a simpler and more constrained model and it is of interest to see whether it also enjoys the privilege to explain the GCE.

The outline of this paper is as follows. We begin by reviewing the Z3SSM and vacuum stability constraints in section 2. Our fit to the GCE is described in section 3, and other relevant constraints are given in section 4. Finally we give our conclusions in section 5.

2 Model

The Z3SSM is the simplest example of semi-annihilating dark matter. The SM is extended by one new particle, a gauge singlet complex scalar S. Its stability is ensured by a global $\mathbb{Z}_3$ symmetry under which it is charged while all SM fields are neutral. This can be the low-energy remnant of a spontaneously broken U(1) gauge symmetry, provided that S is the only light degree of freedom [51]. The Lagrangian is

$$\begin{aligned}\mathcal{L} = \mathcal{L}_{\rm SM} + (\partial_\mu S)^\dagger(\partial^\mu S) - (M_S^2 - \frac{1}{2}\lambda_{\rm HS} v_{EW}^2) S^\dagger S - \frac{\mu_3}{2}\left(S^3 + (S^\dagger)^3\right) \\ - \lambda_{\rm HS}(H^\dagger H)(S^\dagger S) - \frac{1}{2}\lambda_S (S^\dagger S)^2. \end{aligned} \tag{2.1}$$

[1] For other attempts to explain the GCE in SA models, see refs. [46–48].

There are four new parameters: the DM mass M_S, SA coupling μ_3, Higgs portal coupling $\lambda_{\rm HS}$ and quartic λ_S. Of these, μ_3 may be taken real and positive without loss of generality while the quartic couplings are perturbative if $|\lambda_{\rm HS}| < 4\pi$ and $|\lambda_S| < \pi$ [52].

The vacuum stability of this model was studied in ref. [49]. There are four inequivalent vacua, depending on which of H and ϕ acquire VEVs. The desired solution has $\langle\phi\rangle = 0$ to preserve the global $\mathbb{Z}_3$, and $\langle H\rangle \neq 0$ for EWSB. Demanding that this is the global minimum at the weak scale sets the bound

$$\mu_3 \lesssim 2\sqrt{\lambda_S} M_S \leq 2\sqrt{\pi}\, M_S\,. \tag{2.2}$$

The second inequality results from imposing the perturbativity constraint. This is the most robust consistency bound on the SA coupling.[2] Stronger bounds exist when we consider the effects of the renormalisation group. For the values of the Higgs-portal couplings of interest, $\lambda_{\rm HS} \approx 0.05$, large values of λ_S destabilize the vacuum as we run the couplings to a high scale Λ. Requiring that $\Lambda \lesssim 10^9\,\text{GeV}$, i.e. the same scale as the instability in the SM, gives the stronger constraint

$$\lambda_S \lesssim 0.5\,, \qquad \mu_3 \lesssim \sqrt{2}\, M_S\,. \tag{2.3}$$

Aside from these vacuum stability constraints, the DM quartic λ_S has no further effect on the phenomenology, leaving a 3-dimensional parameter space.

3 Galactic center excess

The Planck satellite measured the dark matter density $\Omega_{DM}h^2 \in [0.1126, 0.1246]$ at 3σ [53]. We use micrOMEGAs 4.0 [54] to compute the relic density including the effect of SA, and demand that S saturate this result. This fixes μ_3 as a function of $(M_S, \lambda_{\rm HS})$. In this model, SA decreases the relic abundance, so there is an effective upper bound on $\lambda_{\rm HS}$ as a function of M_S given when the correct relic abundance is obtained for $\mu_3 = 0$. This is the upper grey region in figure 3, for $\lambda_{\rm HS} \gtrsim 0.06$. We also show a lower grey region where we need $\mu_3 > 4000\,\text{GeV}$ to produce the Planck results, and a gold line showing the consistency bound of eq. (2.3).

The differential photon flux from DM annihilation and SA is

$$\frac{d^2\Phi}{d\Omega dE_\gamma} = \frac{1}{8\pi m_S^2} \sum_i \frac{dN_i}{dE_\gamma} \langle\sigma_i v\rangle \int_{l.o.s.} \rho^2 dl\,, \tag{3.1}$$

where ρ is the DM density and the sum i runs over different annihilation and SA channels. The astrophysical dependence of the flux factors out, and is conventionally expressed in terms of

$$\bar{J}(\Delta\Omega) = \frac{1}{\Delta\Omega} \int_{\Delta\Omega} d\Omega \int_{l.o.s.} \rho^2 dl\,. \tag{3.2}$$

We follow ref. [7] and parameterise $\bar{J}$ as

$$\bar{J} = \mathcal{J}\, \bar{J}_{\rm can}\,, \tag{3.3}$$

[2] Allowing this vacuum to be metastable with a sufficiently long lifetime weakens the bound slightly, but does not significantly affect our analysis.

JHEP06(2016)156

where $\bar{J}_{\rm can} = 1.58 \times 10^{24}\,{\rm GeV}^2/{\rm cm}^5$. This value corresponds to a Navarro-Frenk-White (NFW) [55] DM halo profile

$$\rho(r) = \rho_0 \frac{(r/r_s)^{-\gamma}}{(1+r/r_s)^{3-\gamma}}\,, \tag{3.4}$$

with scale radius $r_s = 20$ kpc, slope $\gamma = 1.2$, and local dark matter density $\rho_\odot = 0.4\,{\rm GeV/cm}^3$ at $r = r_\odot = 8.5$ kpc. The integral (3.2) is evaluated over the Fermi region of interest, a $15^\circ \times 15^\circ$ square centered on the galactic center. $\mathcal{J} \in [0.14, 4.0]$ represents our uncertainty in the DM density distribution, derived from the ranges $\gamma = 1.2 \pm 0.1$ and $\rho_\odot = 0.4 \pm 0.2\,{\rm GeV/cm}^3$.

We will find that larger values of $\mathcal{J}$, and hence γ and $\rho_\odot$, are preferred. We note that we could also consider smaller values for the NFW parameters, together with a modest $\mathcal{O}(10)$ boost from DM substructure [56, 57]. The question of whether, and how large, such an enhancement can be is an active area of current research [58–62]. However, we need a much smaller increase than the $\mathcal{O}(10^2$–$10^3)$ boosts usually considered [61], which is more robust to arguments against the existence of such enhancements.

The sum in eq. (3.1) runs over all annihilation processes $S^\dagger S \to SM$, plus the SA process $SS \to S^\dagger h$. We use the PPPC 4 DM ID [63] expressions $f_i(m_{DM}, E_\gamma)$ for the energy distributions. For the SA channel, we use the PPPC results for the hh final state, multiplied by one-half as only a single Higgs is produced. Additionally the Higgs is produced with an energy

$$E_h(m_S) = \frac{3m_S^2 + m_h^2}{4m_S}\,, \tag{3.5}$$

so we use the PPPC distributions for $m_{DM} = E_h$. We may then write the total photon flux as

$$\frac{d\Phi}{dE_\gamma}(E_\gamma) = \frac{\mathcal{J}\,\bar{J}_{\rm can}\Delta\Omega}{8\pi m_S^2}\left(\sum_{i,{\rm ann}} \langle\sigma_i v\rangle\, f_i(m_S, E_\gamma) + \frac{1}{2}\langle\sigma_{SA} v\rangle\, f_{hh}(E_h, E_\gamma)\right). \tag{3.6}$$

The Fermi-LAT collaboration presented a total of eight differential spectra of the residual photon flux after subtracting the interstellar emission and point-source contributions [8]. These correspond to four different models of (background) interstellar emission and two different models for the spectrum of the excess. The interstellar emission models in turn consist of two choices for the spatial distribution of sources within the galaxy, and two different fitting algorithms. The spatial distribution of sources was taken either to follow that of OB-stars (relatively close to the galactic centre) or pulsars (relatively far from the galactic centre), with the expectation that the actual distribution lies between the two. When fitting to the data, the Fermi collaboration considered intensity-scaled and index-scaled models for the background; the former varied the normalisation only, while the latter also varied the spectral index.

The two different choices for the spectra of the excess deserve some discussion. The simpler choice models the excess as a simple power-law with an exponential cut-off as a proxy for either pulsar emission or DM annihilation. The Fermi collaboration also considered a more complex fit where the energy band between 1 and 100 GeV was divided into

JHEP06(2016)156

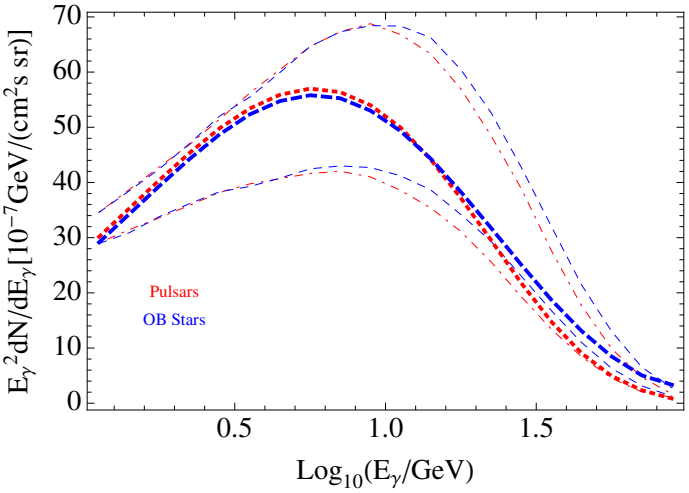

Figure 2. The photon flux for the best-fit point in the Pulsar (OB Stars) intensity-scaled scenario modelled with a single power-law through out all 20 energy bins is shown by the red dotted (blue) line. The Fermi residual spectral bands lie between the fainter red dot-dashed (blue dashed) lines.

ten bins of equal logarithmic size. The spectrum was then fit with a power-law where the overall normalisation *and* the spectral index within each bin were allowed to vary, such that the spectrum is continuous at all points.

We perform a χ^2 analysis on the eight computed photon spectra in 20 bins, assuming a symmetric uncertainty distribution. The quality of the fit improves with increasing $\mathcal{J}$, especially once all constraints are considered. For spectra modelled with a single power-law throughout all energy bins, the best fits are found in the intensity-scaled Pulsars and OB-stars scenarios. The other two, the Pulsars (OB stars) index-scaled scenarios, are too hard for the Z3SSM. The best fit point for the pulsar (OB stars) intensity-scaled scenario with $\mathcal{J} = 4.0$ is $m_S = 125(161)\,\text{GeV}$, $\lambda_{\text{HS}} = 0.0467(0.0548)$, $\mu_3 = 52.7(64.5)\,\text{GeV}$ and $\chi^2 = 2.4(2.1)$. We show the flux at these points together with the GCE spectra in figure 2, and the 1, 2 and 3σ contours in figure 3.

As for the spectra modelled with a different power-law in each energy bin, only one can be reasonably fit with the Z3SSM: the index-scaled Pulsar scenario. The remaining three are too soft. The fit here is worse, but the best fit point has $\chi^2 = 16.1/20$ d.o.f. (for $\mathcal{J} = 4.0$ and $m_S = 132\,\text{GeV}$, $\lambda_{\text{HS}} = 0.0335$, and $\mu_3 = 86.7\,\text{GeV}$). We show the 1, 2 and 3σ contours and the best-fit photon flux in figure 4. The phenomenology of this case is otherwise very similar to the two shown in figure 3.

Except the ones shown in figure 2 and figure 3, the fits with the other five spectra presented by the Fermi collaboration all have $\chi^2/\text{d.o.f.} \gtrsim 4$. The best fit points are characterised by a strong annihilation signal and a relatively small SA cross section. The contribution of the different final states $WW : ZZ : hh : S^\dagger h \approx 69\% : 29\% : 1.2\% : 0.43\%(45\% : 20\% : 27\% : 8.0\%)$ for Pulsars (OB stars). This arises as the SA cross section is bound by the perturbativity constraints on μ_3. However, SA still plays an important role in setting the relic density for smaller λ_{HS}, and thus avoiding direct detection constraints.

JHEP06(2016)156

4 Additional constraints

An unavoidable constraint for any potential explanation of the GCE comes from Fermi observations of dwarf spheroidal galaxies (dSphs) [64, 65]. These are DM-dominated objects offering low backgrounds and reasonably well-understood density distributions. The same experiment that observed the GCE has seen no corresponding excess from these sources.

The most recent limits from Fermi [66] are given in terms of cross sections to various SM final states. Our model (semi-)annihilates to several different final states, so to apply these limits we make two simplifications. We assume that the differences between the spectra for WW, ZZ and $h(h)$ are sufficiently small that they do not significantly effect the constraints. Further, since the SA channel is sub-dominant and the GCE preferred region is for $m_S \approx m_h$, we neglect the effects of the different Higgs boost of eq. (3.5). This gives us the bound

$$\sum_{i,\text{ann}} \langle \sigma_i v \rangle + \frac{1}{2} \langle \sigma_{SA} v \rangle < \sigma v^{dSphs,WW} . \tag{4.1}$$

We show the resultant upper bound on λ_{HS} in figures 3 and 4 in pink. We see that for $\mathcal{J} = 4$, the best-fit region is not excluded. However, smaller values $\mathcal{J} \lesssim 3$ start to be in tension. This is in line with other studies that have found that the GCE and dSph bounds are consistent only for an enhanced signal from the galactic center [65].

Limits from collider searches and direct detection are independent of SA (and μ_3), and similar to bounds on for a scalar singlet $\mathbb{Z}_2$ model. Collider searches in monojets and jets + MET set no current bounds in the mass range of interest, and are not expected to be constraining in the near future [45, 67, 68].

Direct detection bounds in contrast are very relevant. The spin-independent scattering cross section is

$$\sigma_{\text{SI}}(SN \to SN) = \frac{\lambda_{\text{HS}}^2 f_N^2}{4\pi} \frac{m_N^4}{m_H^4 (m_N + M_S)^2} , \tag{4.2}$$

where f_N is the Higgs-nucleon coupling

$$f_N = \sum_q f_q = \sum_q \frac{m_q}{m_N} \langle N | \bar{q} q | N \rangle , \tag{4.3}$$

and $m_N = 0.946\,\text{GeV}$. We follow ref. [69] and take $f_N = 0.345$ in placing our limits. See refs. [69–78] for more details. The strongest spin-independent scattering limits for DM masses $\gtrsim 5\,\text{GeV}$ are from the preliminary run at LUX [79]. For $m_S = 140\,\text{GeV}$, LUX excludes $\sigma_n > 1.7 \times 10^{-45}\ \text{cm}^2$. We plot the resultant upper limits in figures 3 and 4 in orange. For $m_S < m_h$, these are the most stringent limits on λ_{HS}.

5 Conclusions

In this paper, we studied the simplest example of semi-annihilating DM, the Z3SSM, in the context of the Fermi GCE. The Z3SSM has only three parameters relevant to DM phenomenology; we reduce this to a two-dimensional parameter space by demanding the relic density reproduce observations. Our main result is given in figures 3 and 4, which

JHEP06(2016)156

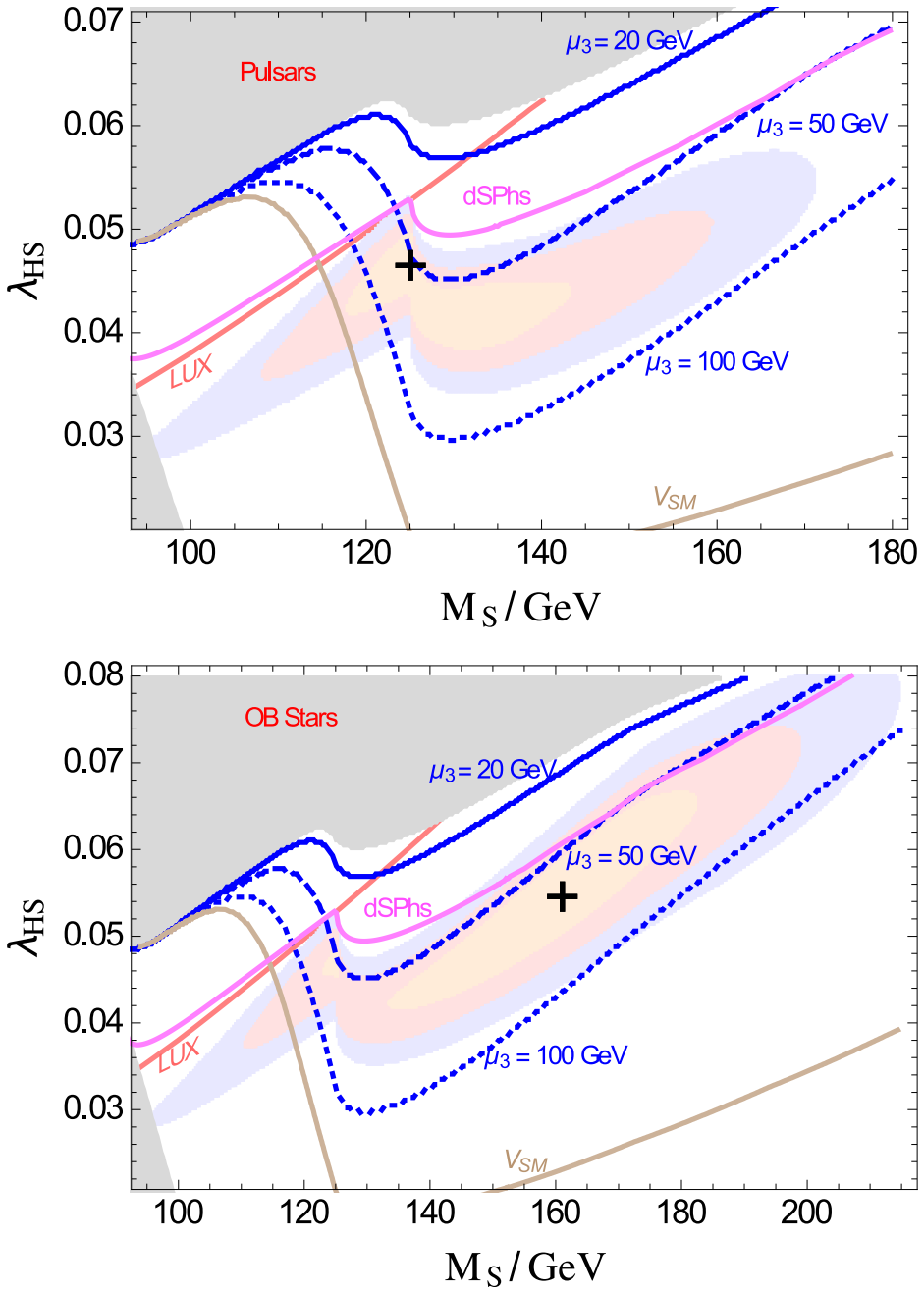

Figure 3. Preferred region for the GCE with experimental and theoretical constraints in the M_S–$\lambda_{\rm HS}$ plane for two interstellar emission scenarios, Pulsars intensity-scaled (upper panel) and OB Stars intensity-scaled (lower panel), modelled with a single power-law throughout all 20 energy bins. In the grey regions, no value of $\mu_3 \in [0, 4000]$ GeV could reproduce the observed relic density. Contours of μ_3 are in blue, with the gold line labelled $V_{\rm SM}$ denoting the stability bound of eq. (2.3). The black cross marks the GCE best-fit point, and the yellow, red and blue shaded ellipses the 1, 2 and 3-σ contours. The regions excluded by LUX and by Fermi observations of dSphs, as discussed in section 4, are above and to the left of the labelled contours.

JHEP06(2016)156

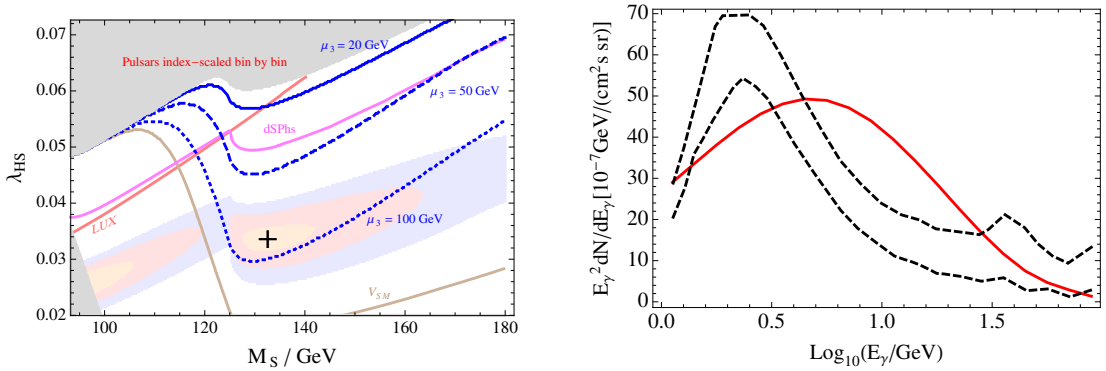

Figure 4. (Left): preferred region for the GCE with experimental and theoretical constraints in the M_S–$\lambda_{\rm HS}$ plane for the Pulsars index-scaled interstellar emission scenario modelled with a different power-law in each energy bin. The different regions are labelled with the same conventions as in figure 3. (Right): photon flux for the best-fit point lablled as a black cross in the left panel. The Fermi residual spectral bands modelled with a different power-law bin by bin are shown in black dashed lines.

show the best-fit regions as well as constraints from direct detection, dwarf spheroidals and vacuum stability.

We find that, assuming the signal from the galactic centre is at the higher range of expectations for an NFW profile, this model *can* explain the GCE while remaining consistent with all current constraints. The agreement with the measured spectral excess is quite good for a 20-bin analysis with $\chi^2 = 2.1$ at the best fit point and spectrum. SA is a subdominant contribution to the γ-ray flux, but plays an essential role in obtaining the correct relic density and easing bounds from LUX and from dwarf spheroidals. This model can provide good fits to three of the different residual spectra presented by Fermi. The best fit is when the excess is modelled as a single power-law through out 20 energy bins, and interstellar gamma-ray emission is accounted for with intensity-scaled Pulsar or OB-star models; a weaker fit is possible for a spectra modelled with different power-law in each bin and an index-scaled Pulsar background. Other spectra presented by Fermi are either too hard to too soft to be reproduced.

Finally, we note that the region where this model explains the GCE only marginally evades the current bounds. Moderate improvements in either type of limit should exclude or, more optimistically, discover the region of parameter space discussed here. In particular, the full LUX results are expected to improve the direct detection bounds by a factor of ~ 5 in the relevant mass range [80]. Thus we expect this explanation of the GCE to be proved or falfisied soon.

Acknowledgments

AS would like to thank the Instituto de Fisica Teorica (IFT UAM-CSIC) in Madrid for its support via the Centro de Excelencia Severo Ochoa Program under Grant SEV-2012-0249, during the IBS-Multidark Joint Workshop on Dark Matter, where part of this work

JHEP06(2016)156

was completed. YC was supported by the Australian Research Council. This work was supported by IBS under the project code, IBS-R018-D1.

References

[1] D. Hooper and L. Goodenough, *Dark matter annihilation in the Galactic Center as seen by the Fermi Gamma Ray Space telescope*, *Phys. Lett.* **B 697** (2011) 412 [arXiv:1010.2752] [INSPIRE].

[2] A. Boyarsky, D. Malyshev and O. Ruchayskiy, *A comment on the emission from the Galactic Center as seen by the Fermi telescope*, *Phys. Lett.* **B 705** (2011) 165 [arXiv:1012.5839] [INSPIRE].

[3] D. Hooper and T. Linden, *On the origin of the gamma rays from the Galactic Center*, *Phys. Rev.* **D 84** (2011) 123005 [arXiv:1110.0006] [INSPIRE].

[4] K.N. Abazajian and M. Kaplinghat, *Detection of a gamma-ray source in the Galactic Center consistent with extended emission from dark matter annihilation and concentrated astrophysical emission*, *Phys. Rev.* **D 86** (2012) 083511 [*Erratum ibid.* **D 87** (2013) 129902] [arXiv:1207.6047] [INSPIRE].

[5] T. Daylan et al., *The characterization of the gamma-ray signal from the central Milky Way: a case for annihilating dark matter*, *Phys. Dark Univ.* **12** (2016) 1 [arXiv:1402.6703] [INSPIRE].

[6] F. Calore, I. Cholis and C. Weniger, *Background model systematics for the Fermi GeV excess*, *JCAP* **03** (2015) 038 [arXiv:1409.0042] [INSPIRE].

[7] P. Agrawal, B. Batell, P.J. Fox and R. Harnik, *WIMPs at the Galactic Center*, *JCAP* **05** (2015) 011 [arXiv:1411.2592] [INSPIRE].

[8] Fermi-LAT collaboration, M. Ajello et al., *Fermi-LAT observations of high-energy γ-ray emission toward the Galactic Center*, *Astrophys. J.* **819** (2016) 44 [arXiv:1511.02938] [INSPIRE].

[9] F. Calore, I. Cholis, C. McCabe and C. Weniger, *A tale of tails: dark matter interpretations of the Fermi GeV excess in light of background model systematics*, *Phys. Rev.* **D 91** (2015) 063003 [arXiv:1411.4647] [INSPIRE].

[10] J.M. Cline, G. Dupuis, Z. Liu and W. Xue, *Multimediator models for the Galactic Center gamma ray excess*, *Phys. Rev.* **D 91** (2015) 115010 [arXiv:1503.08213] [INSPIRE].

[11] J.D. Ruiz-Alvarez, C.A. de S. Pires, F.S. Queiroz, D. Restrepo and P.S. Rodrigues da Silva, *On the connection of gamma-rays, dark matter and Higgs searches at LHC*, *Phys. Rev.* **D 86** (2012) 075011 [arXiv:1206.5779] [INSPIRE].

[12] C. Boehm, M.J. Dolan, C. McCabe, M. Spannowsky and C.J. Wallace, *Extended gamma-ray emission from Coy Dark Matter*, *JCAP* **05** (2014) 009 [arXiv:1401.6458] [INSPIRE].

[13] A. Alves, S. Profumo, F.S. Queiroz and W. Shepherd, *Effective field theory approach to the Galactic Center gamma-ray excess*, *Phys. Rev.* **D 90** (2014) 115003 [arXiv:1403.5027] [INSPIRE].

JHEP06(2016)156

[14] A. Berlin, D. Hooper and S.D. McDermott, *Simplified dark matter models for the Galactic Center gamma-ray excess*, *Phys. Rev.* **D 89** (2014) 115022 [arXiv:1404.0022] [INSPIRE].

[15] P. Agrawal, B. Batell, D. Hooper and T. Lin, *Flavored dark matter and the Galactic Center gamma-ray excess*, *Phys. Rev.* **D 90** (2014) 063512 [arXiv:1404.1373] [INSPIRE].

[16] C. Boehm, M.J. Dolan and C. McCabe, *A weighty interpretation of the Galactic Centre excess*, *Phys. Rev.* **D 90** (2014) 023531 [arXiv:1404.4977] [INSPIRE].

[17] M. Abdullah, A. DiFranzo, A. Rajaraman, T.M.P. Tait, P. Tanedo and A.M. Wijangco, *Hidden on-shell mediators for the Galactic Center γ-ray excess*, *Phys. Rev.* **D 90** (2014) 035004 [arXiv:1404.6528] [INSPIRE].

[18] A. Martin, J. Shelton and J. Unwin, *Fitting the Galactic Center gamma-ray excess with cascade annihilations*, *Phys. Rev.* **D 90** (2014) 103513 [arXiv:1405.0272] [INSPIRE].

[19] T. Mondal and T. Basak, *Class of Higgs-portal Dark Matter models in the light of gamma-ray excess from Galactic center*, *Phys. Lett.* **B 744** (2015) 208 [arXiv:1405.4877] [INSPIRE].

[20] L. Wang and X.-F. Han, *A simplified 2HDM with a scalar dark matter and the galactic center gamma-ray excess*, *Phys. Lett.* **B 739** (2014) 416 [arXiv:1406.3598] [INSPIRE].

[21] C. Balázs and T. Li, *Simplified dark matter models confront the gamma ray excess*, *Phys. Rev.* **D 90** (2014) 055026 [arXiv:1407.0174] [INSPIRE].

[22] M. Cahill-Rowley, J. Gainer, J. Hewett and T. Rizzo, *Towards a supersymmetric description of the Fermi Galactic Center excess*, *JHEP* **02** (2015) 057 [arXiv:1409.1573] [INSPIRE].

[23] M. Heikinheimo and C. Spethmann, *Galactic centre GeV photons from dark technicolor*, *JHEP* **12** (2014) 084 [arXiv:1410.4842] [INSPIRE].

[24] K. Ghorbani and H. Ghorbani, *Scalar split WIMPs in future direct detection experiments*, *Phys. Rev.* **D 93** (2016) 055012 [arXiv:1501.00206] [INSPIRE].

[25] A. Biswas, D. Majumdar and P. Roy, *Nonthermal two component dark matter model for Fermi-LAT γ-ray excess and 3.55 keV X-ray line*, *JHEP* **04** (2015) 065 [arXiv:1501.02666] [INSPIRE].

[26] M. Kaplinghat, T. Linden and H.-B. Yu, *Galactic Center excess in γ rays from annihilation of self-interacting dark matter*, *Phys. Rev. Lett.* **114** (2015) 211303 [arXiv:1501.03507] [INSPIRE].

[27] A. Achterberg, S. Amoroso, S. Caron, L. Hendriks, R. Ruiz de Austri and C. Weniger, *A description of the Galactic Center excess in the Minimal Supersymmetric Standard Model*, *JCAP* **08** (2015) 006 [arXiv:1502.05703] [INSPIRE].

[28] G. Elor, N.L. Rodd and T.R. Slatyer, *Multistep cascade annihilations of dark matter and the Galactic Center excess*, *Phys. Rev.* **D 91** (2015) 103531 [arXiv:1503.01773] [INSPIRE].

[29] K. Ghorbani and H. Ghorbani, *Two-portal dark matter*, *Phys. Rev.* **D 91** (2015) 123541 [arXiv:1504.03610] [INSPIRE].

[30] A.J. Williams, *Explaining the Fermi Galactic Centre excess in the CMSSM*, arXiv:1510.00714 [INSPIRE].

[31] M. Duerr, P. Fileviez Pérez and J. Smirnov, *Gamma-ray excess and the Minimal Dark Matter Model*, *JHEP* **06** (2016) 008 [arXiv:1510.07562] [INSPIRE].

[32] N. Mirabal, *Dark matter vs. pulsars: catching the impostor*, *Mon. Not. Roy. Astron. Soc.* **436** (2013) 2461 [arXiv:1309.3428] [INSPIRE].

JHEP06(2016)156

[33] K.N. Abazajian, N. Canac, S. Horiuchi and M. Kaplinghat, *Astrophysical and dark matter interpretations of extended gamma-ray emission from the Galactic Center*, *Phys. Rev.* **D 90** (2014) 023526 [arXiv:1402.4090] [INSPIRE].

[34] Q. Yuan and B. Zhang, *Millisecond pulsar interpretation of the Galactic Center γ-ray excess*, *JHEAp* **3-4** (2014) 1 [arXiv:1404.2318] [INSPIRE].

[35] J. Petrović, P.D. Serpico and G. Zaharijas, *Millisecond pulsars and the Galactic Center γ-ray excess: the importance of luminosity function and secondary emission*, *JCAP* **02** (2015) 023 [arXiv:1411.2980] [INSPIRE].

[36] R.M. O'Leary, M.D. Kistler, M. Kerr and J. Dexter, *Young pulsars and the Galactic Center GeV γ-ray excess*, arXiv:1504.02477 [INSPIRE].

[37] R. Bartels, S. Krishnamurthy and C. Weniger, *Strong support for the millisecond pulsar origin of the Galactic center GeV excess*, *Phys. Rev. Lett.* **116** (2016) 051102 [arXiv:1506.05104] [INSPIRE].

[38] S.K. Lee, M. Lisanti, B.R. Safdi, T.R. Slatyer and W. Xue, *Evidence for unresolved γ-ray point sources in the inner galaxy*, *Phys. Rev. Lett.* **116** (2016) 051103 [arXiv:1506.05124] [INSPIRE].

[39] J. Petrović, P.D. Serpico and G. Zaharijaš, *Galactic Center γ-ray "excess" from an active past of the Galactic Centre?*, *JCAP* **10** (2014) 052 [arXiv:1405.7928] [INSPIRE].

[40] C. Gordon and O. Macias, *Can cosmic rays interacting with molecular clouds explain the Galactic Center γ-ray excess?*, PoS(CRISM2014)042 [arXiv:1410.7840] [INSPIRE].

[41] I. Cholis, C. Evoli, F. Calore, T. Linden, C. Weniger and D. Hooper, *The Galactic Center GeV excess from a series of leptonic cosmic-ray outbursts*, *JCAP* **12** (2015) 005 [arXiv:1506.05119] [INSPIRE].

[42] D. Hooper, I. Cholis, T. Linden, J. Siegal-Gaskins and T. Slatyer, *Pulsars cannot account for the inner galaxy's GeV excess*, *Phys. Rev.* **D 88** (2013) 083009 [arXiv:1305.0830] [INSPIRE].

[43] I. Cholis, D. Hooper and T. Linden, *Challenges in explaining the Galactic Center γ-ray excess with millisecond pulsars*, *JCAP* **06** (2015) 043 [arXiv:1407.5625] [INSPIRE].

[44] T. Linden, *Known radio pulsars do not contribute to the Galactic Center γ-ray excess*, *Phys. Rev.* **D 93** (2016) 063003 [arXiv:1509.02928] [INSPIRE].

[45] Y. Cai and A.P. Spray, *Fermionic semi-annihilating dark matter*, *JHEP* **01** (2016) 087 [arXiv:1509.08481] [INSPIRE].

[46] P. Ko and Y. Tang, *Galactic center γ-ray excess in hidden sector DM models with dark gauge symmetries: local Z_3 symmetry as an example*, *JCAP* **01** (2015) 023 [arXiv:1407.5492] [INSPIRE].

[47] J. Guo, Z. Kang, P. Ko and Y. Orikasa, *Accidental dark matter: case in the scale invariant local B-L model*, *Phys. Rev.* **D 91** (2015) 115017 [arXiv:1502.00508] [INSPIRE].

[48] N. Fonseca, L. Necib and J. Thaler, *Dark matter, shared asymmetries and galactic γ ray signals*, *JCAP* **02** (2016) 052 [arXiv:1507.08295] [INSPIRE].

[49] G. Bélanger, K. Kannike, A. Pukhov and M. Raidal, *Z_3 scalar singlet dark matter*, *JCAP* **01** (2013) 022 [arXiv:1211.1014] [INSPIRE].

[50] V. Silveira and A. Zee, *Scalar phantoms*, *Phys. Lett.* **B 161** (1985) 136 [INSPIRE].

JHEP06(2016)156

[51] P. Ko and Y. Tang, *Self-interacting scalar dark matter with local Z_3 symmetry*, *JCAP* **05** (2014) 047 [arXiv:1402.6449] [INSPIRE].

[52] R.N. Lerner and J. McDonald, *Gauge singlet scalar as inflaton and thermal relic dark matter*, *Phys. Rev.* **D 80** (2009) 123507 [arXiv:0909.0520] [INSPIRE].

[53] PLANCK collaboration, R. Adam et al., *Planck 2015 results. I. Overview of products and scientific results*, arXiv:1502.01582 [INSPIRE].

[54] G. Bélanger, F. Boudjema, A. Pukhov and A. Semenov, *MicrOMEGAs4.1: two dark matter candidates*, *Comput. Phys. Commun.* **192** (2015) 322 [arXiv:1407.6129] [INSPIRE].

[55] J.F. Navarro, C.S. Frenk and S.D.M. White, *The structure of cold dark matter halos*, *Astrophys. J.* **462** (1996) 563 [astro-ph/9508025] [INSPIRE].

[56] P. Brun, T. Delahaye, J. Diemand, S. Profumo and P. Salati, *The cosmic ray lepton puzzle in the light of cosmological N-body simulations*, *Phys. Rev.* **D 80** (2009) 035023 [arXiv:0904.0812] [INSPIRE].

[57] J.M. Cline, A.C. Vincent and W. Xue, *Leptons from dark matter annihilation in Milky Way subhalos*, *Phys. Rev.* **D 81** (2010) 083512 [arXiv:1001.5399] [INSPIRE].

[58] S. Profumo, K. Sigurdson and M. Kamionkowski, *What mass are the smallest protohalos?*, *Phys. Rev. Lett.* **97** (2006) 031301 [astro-ph/0603373] [INSPIRE].

[59] L. Pieri, J. Lavalle, G. Bertone and E. Branchini, *Implications of high-resolution simulations on indirect dark matter searches*, *Phys. Rev.* **D 83** (2011) 023518 [arXiv:0908.0195] [INSPIRE].

[60] R. Bartels and S. Ando, *Boosting the annihilation boost: tidal effects on dark matter subhalos and consistent luminosity modeling*, *Phys. Rev.* **D 92** (2015) 123508 [arXiv:1507.08656] [INSPIRE].

[61] A.N. Baushev, *Can the dark matter annihilation signal be significantly boosted by substructures?*, *JCAP* **01** (2016) 018 [arXiv:1506.08609] [INSPIRE].

[62] F.C. van den Bosch, F. Jiang, D. Campbell and P. Behroozi, *On the segregation of dark matter substructure*, *Mon. Not. Roy. Astron. Soc.* **455** (2016) 158 [arXiv:1510.01586] [INSPIRE].

[63] M. Cirelli et al., *PPPC 4 DM ID: a poor particle physicist cookbook for dark matter indirect detection*, *JCAP* **03** (2011) 051 [*Erratum ibid.* **1210** (2012) E01] [arXiv:1012.4515] [INSPIRE].

[64] A. Geringer-Sameth, S.M. Koushiappas and M.G. Walker, *Comprehensive search for dark matter annihilation in dwarf galaxies*, *Phys. Rev.* **D 91** (2015) 083535 [arXiv:1410.2242] [INSPIRE].

[65] K.N. Abazajian and R.E. Keeley, *Bright gamma-ray Galactic Center excess and dark dwarfs: Strong tension for dark matter annihilation despite Milky Way halo profile and diffuse emission uncertainties*, *Phys. Rev.* **D 93** (2016) 083514 [arXiv:1510.06424] [INSPIRE].

[66] FERMI-LAT collaboration, M. Ackermann et al., *Searching for dark matter annihilation from Milky Way dwarf spheroidal galaxies with six years of Fermi Large Area Telescope Data*, *Phys. Rev. Lett.* **115** (2015) 231301 [arXiv:1503.02641] [INSPIRE].

[67] M. Endo and Y. Takaesu, *Heavy WIMP through Higgs portal at the LHC*, *Phys. Lett.* **B 743** (2015) 228 [arXiv:1407.6882] [INSPIRE].

JHEP06(2016)156

[68] N. Craig, H.K. Lou, M. McCullough and A. Thalapillil, *The Higgs portal above threshold*, *JHEP* **02** (2016) 127 [arXiv:1412.0258] [INSPIRE].

[69] J.M. Cline, K. Kainulainen, P. Scott and C. Weniger, *Update on scalar singlet dark matter*, *Phys. Rev.* **D 88** (2013) 055025 [arXiv:1306.4710] [INSPIRE].

[70] J.M. Alarcon, J. Martin Camalich and J.A. Oller, *The chiral representation of the πN scattering amplitude and the pion-nucleon sigma term*, *Phys. Rev.* **D 85** (2012) 051503 [arXiv:1110.3797] [INSPIRE].

[71] J.M. Alarcon, J. Martin Camalich and J.A. Oller, *Improved description of the πN-scattering phenomenology in covariant baryon chiral perturbation theory*, *Annals Phys.* **336** (2013) 413 [arXiv:1210.4450] [INSPIRE].

[72] P. Junnarkar and A. Walker-Loud, *Scalar strange content of the nucleon from lattice QCD*, *Phys. Rev.* **D 87** (2013) 114510 [arXiv:1301.1114] [INSPIRE].

[73] J.R. Ellis, K.A. Olive and C. Savage, *Hadronic uncertainties in the elastic scattering of supersymmetric dark matter*, *Phys. Rev.* **D 77** (2008) 065026 [arXiv:0801.3656] [INSPIRE].

[74] Y. Akrami, C. Savage, P. Scott, J. Conrad and J. Edsjo, *How well will ton-scale dark matter direct detection experiments constrain minimal supersymmetry?*, *JCAP* **04** (2011) 012 [arXiv:1011.4318] [INSPIRE].

[75] G. Bertone, D.G. Cerdeno, M. Fornasa, R. Ruiz de Austri, C. Strege and R. Trotta, *Global fits of the CMSSM including the first LHC and XENON100 data*, *JCAP* **01** (2012) 015 [arXiv:1107.1715] [INSPIRE].

[76] A. Crivellin, M. Hoferichter and M. Procura, *Accurate evaluation of hadronic uncertainties in spin-independent WIMP-nucleon scattering: Disentangling two- and three-flavor effects*, *Phys. Rev.* **D 89** (2014) 054021 [arXiv:1312.4951] [INSPIRE].

[77] M. Hoferichter, J. Ruiz de Elvira, B. Kubis and U.-G. Meißner, *High-precision determination of the pion-nucleon σ term from Roy-Steiner equations*, *Phys. Rev. Lett.* **115** (2015) 092301 [arXiv:1506.04142] [INSPIRE].

[78] J.M. Alarcon, L.S. Geng, J. Martin Camalich and J.A. Oller, *The strangeness content of the nucleon from effective field theory and phenomenology*, *Phys. Lett.* **B 730** (2014) 342 [arXiv:1209.2870] [INSPIRE].

[79] LUX collaboration, D.S. Akerib et al., *First results from the LUX dark matter experiment at the Sanford Underground Research Facility*, *Phys. Rev. Lett.* **112** (2014) 091303 [arXiv:1310.8214] [INSPIRE].

[80] LUX collaboration, M. Szydagis et al., *A detailed look at the first results from the Large Underground Xenon (LUX) dark matter experiment*, in 10^{th} *International Symposium on Cosmology and Particle Astrophysics (CosPA 2013)*, November 12–15, Honolulu, Hawaii, U.S.A. (2014), arXiv:1402.3731 [INSPIRE].

JHEP06(2016)156